

FINITE ELEMENT MODELING AND EXPERIMENTAL VALIDATION OF BUCKLE ARRESTORS FOR DEEPWATER PIPELINES.

Luciano O. Mantovano, Pablo Amenta, Roberto Charreau, Daniel Johnson, Andrea Assanelli and Rita G. Toscano

Center for Industrial Research (CINI), Tenaris
Dr. Jorge A. Simini 250,
B2804MHA, Campana, Argentina.
e-mail: rtoscano@rtenaris.com, web page: <http://www.fudetec.com>

Keywords: Collapse, Crossover, Pipelines, Arrestors.

Abstract. *Deepwater pipelines are designed to withstand, without collapsing, the external pressure acting on them and the bending imposed on them, either by the laying process or by the topology of the sea bottom. In previous publications we have developed and experimentally validated finite element models to predict collapse loads and collapse propagation loads.*

Even though a pipeline normally has enough strength to prevent collapse under normal operation conditions, under some accidental conditions collapse may occur at some section. Being the collapse propagation pressure much lower than the collapse pressure, the collapse, once it occurs, may propagate through large distances along the pipeline. To avoid the occurrence of this propagation, collapse arrestors are normally welded to pipelines and, if the cross-over pressure is higher than the external pressure, they prevent the collapse propagation.

The accurate and reliable determination, using finite element models, of cross-over pressures, for different combinations pipes / arrestors, is a key engineering capability.

In this paper we discuss the finite element models that we developed, using shell elements, for the calculation of cross over pressures and their experimental validation for seamless steel pipes.

In the literature two cross-over mechanisms were identified: the flattening and the flipping modes; their occurrence depends on the ratio (arrestors stiffness/pipes stiffness). Numerical and experimental results that we obtained for the two cases are compared and we show that the agreement between them for both, cross-over pressure and cross-over mechanism, is excellent.

1 INTRODUCTION

Deepwater pipelines are normally subjected to external pressure and bending. They fail due to structural collapse when the external loading exceeds the pipes collapse limit surface. For seamless steel pipes, the influence on this limit surface of manufacturing imperfections has been thoroughly studied using finite element models that have been validated via laboratory full-scale tests ([Assanelli et al. 2000](#) ; [Toscano et al. 2002](#); [Toscano et al. 2003a, b, c](#); [Toscano et al. 2004](#))

If by accident the collapse is initiated at a certain location, the collapse is either restrained to the collapse initiation section or it propagates along the pipeline, being this second alternative the most detrimental one for the pipeline integrity. ([Palmer and Martin, 1975](#)) Since the external collapse propagation pressure is usually quite low in comparison with the external collapse pressure, it is necessary to build in the pipeline spaced reinforcements, usually steel rings, to act as arrestors for the collapse propagation.

Two different buckle arrestor cross-over mechanisms were identified in the literature: flattening and flipping. The occurrence of either cross-over mechanism is determined by the geometry of the pipes and of the arrestors. ([Park and Kyriakides, 1997](#)) In this paper we develop finite element models to analyze the collapse pressure, collapse propagation pressure and cross-over pressure of pipelines and we present an experimental validation for these models.

2 EXPERIMENTAL RESULTS USING SEAMLESS STEEL PIPES

Few experimental results are available in the literature for the cross-over of integral ring buckle arrestors under external pressure on large diameter carbon steel pipes. ([Johns, Mesloh and Sorenson, 1978](#); [Langer, 1999](#)) Most of the available experimental results correspond to stainless steel and small diameter steel pipes. ([Park and Kyriakides, 1997](#); [Kyriakides et al. 1998](#); [Netto and Kyriakides, 2000a,b](#); [Netto and Estefen, 1996](#)) Therefore this paper adds to the available technical literature in a range where more information can be useful.

The purpose of our laboratory tests was to determine the equilibrium path for the assembly (pipe + arrestor + pipe) under external pressure; and from it determine the collapse pressure, and the cross-over pressure. Fig. 1 shows the sample configuration.

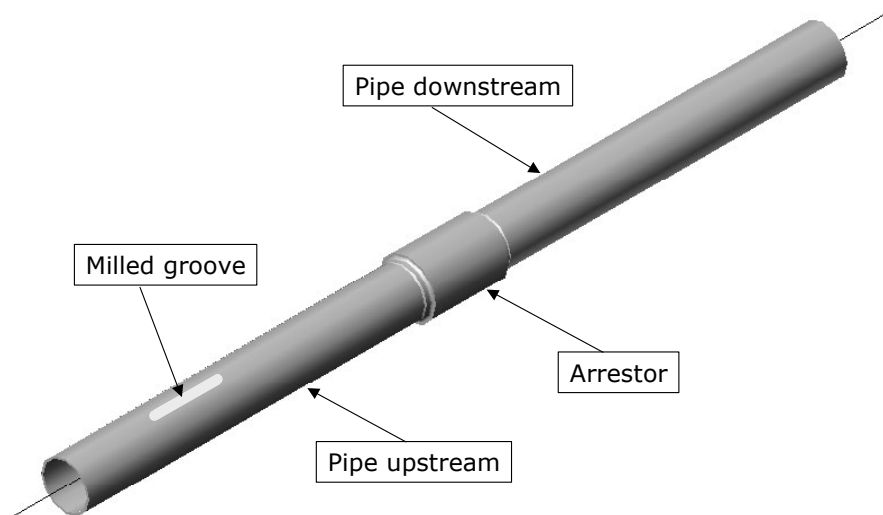


Figure 1. Sample configuration.

We examined the behaviour of six different integral-ring buckle arrestor configurations welded on 141.3 mm (5 9/16") seamless pipe. The arrestors were machined from a thicker seamless pipe (O.D. = 168.27 mm (6 5/8") and wall thickness 21.95 mm) to various lengths and wall thickness, but their I.D. was made to match those of the pipes welded to them. To localize the buckle initiation we milled a groove in one of the pipes (upstream pipe). In Fig. 2 we present a detail of the arrestors:

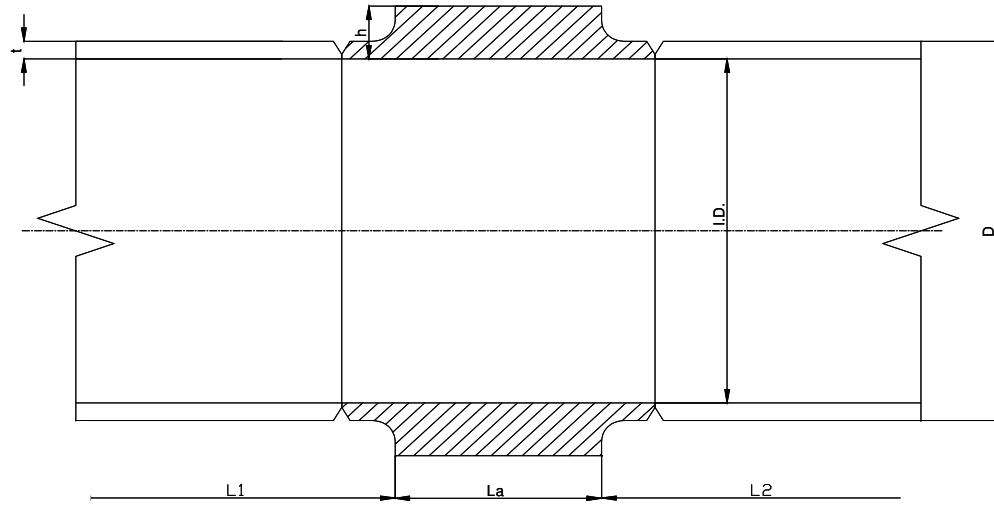


Figure 2. Arrestor geometry.

Table 1 provides the data for the six tested samples:

Sample	Pipe OD [mm]	Pipe thickness (t) [mm]	Pipe steel grade	Arrestor (h/t)	Arrestor (La/D)	Arrestor steel grade	Sample length [mm]	Expected cross-over mechanism
1	141.3	6.55	X42	3.0	1.50	6 (ASTM A-333)	2300	Flipping
2	141.3	6.55	X42	2.0	0.50	6 (ASTM A-333)	2250	Flattening
3	141.3	6.55	X42	3.0	0.50	6 (ASTM A-333)	2240	Flattening
4	141.3	6.55	X42	2.5	0.50	X42	2250	Flattening
5	141.3	6.55	X42	3.0	0.75	X42	2274	Flipping
6	141.3	6.55	X42	3.0	1.00	X42	2330	Flipping

Table 1. Data for tested samples

2.1 Geometrical Characterization of the Tested Samples

The outer surface of the samples was mapped using the *shapemeter* (Assanelli et al. 2000); the corresponding Fourier decomposition of one of the tested samples is shown in Fig. 3. The zone with high amplitude corresponds to the milled groove, whereas the zone with low amplitude belongs to the arrestor, which was machined in a lathe.

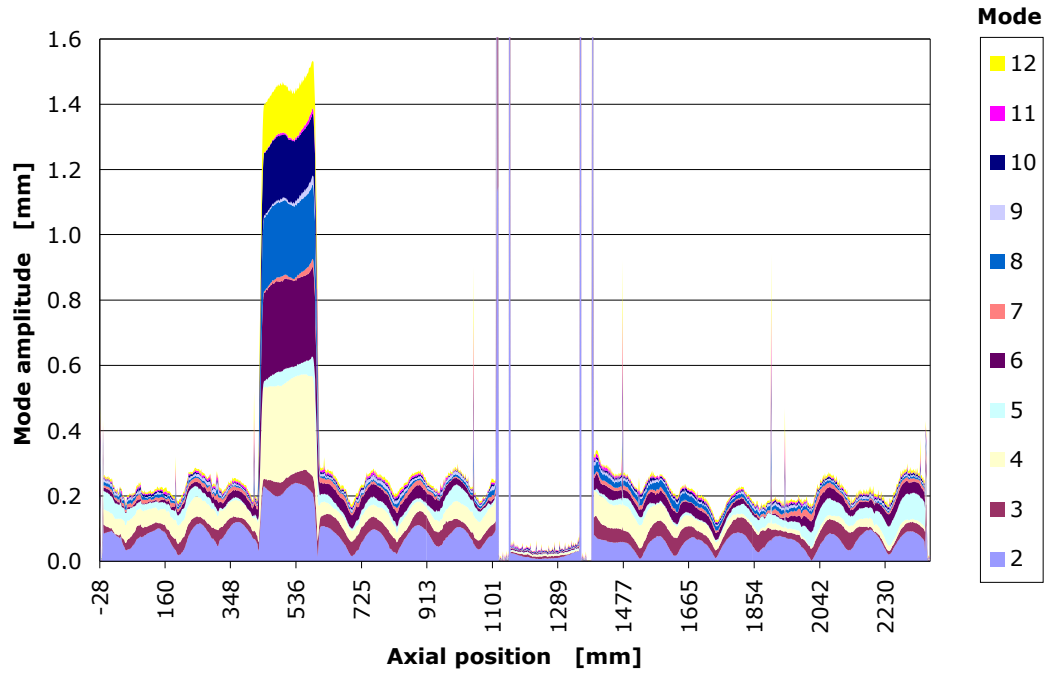


Figure 3. OD Fourier analysis of the first sample.

The thickness of the samples was also mapped using a standard ultrasonic gauge; the corresponding thickness map of the first sample is shown in Fig. 4.

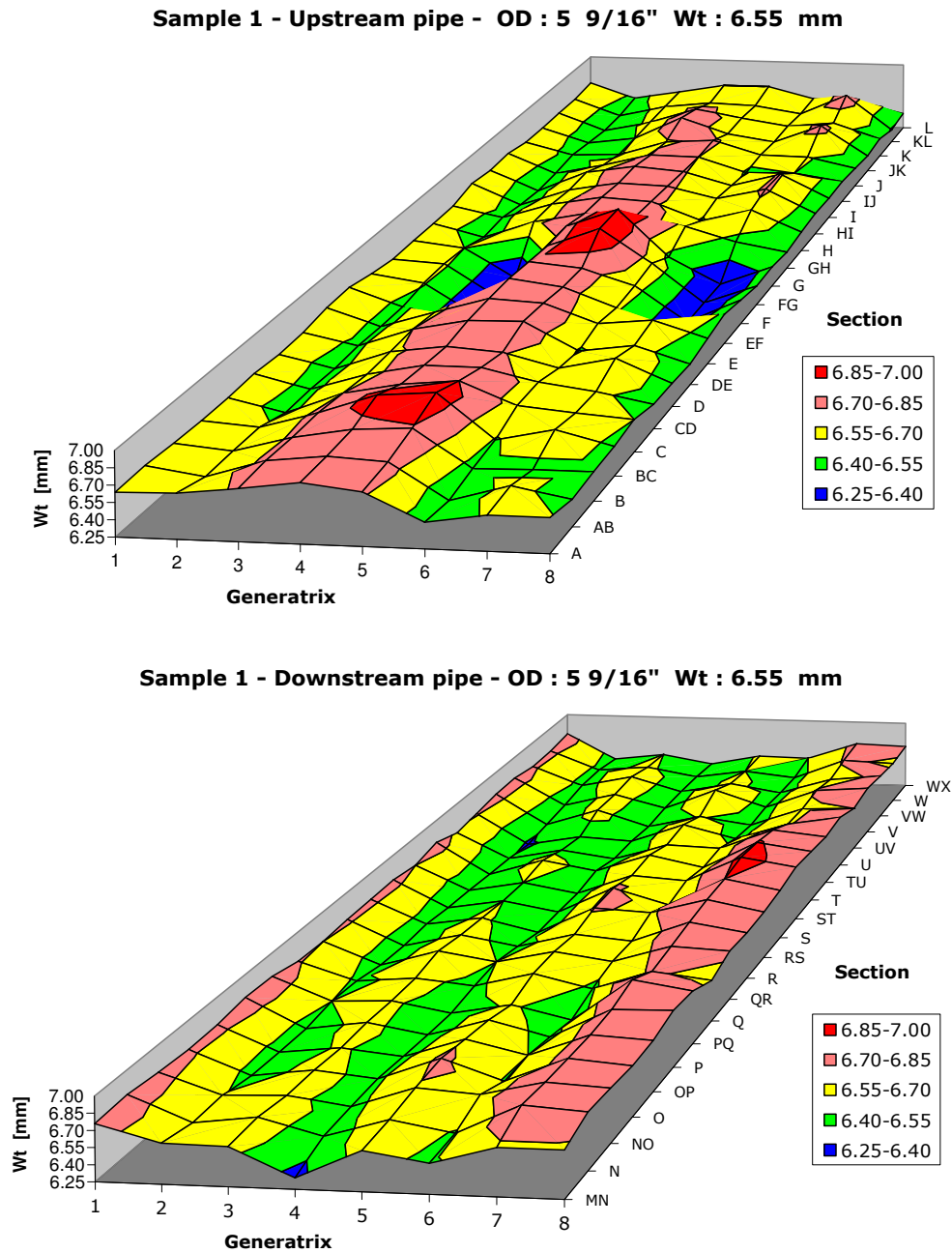


Figure 4. Thickness distribution for the first sample.

2.2 Mechanical Characterization of the Tested Samples

For all the pipe and arrestor materials we determined:

- The yield stress as an average of several measurements and the engineering stress – engineering strain curves (longitudinal tensile tests since the thickness of the pipes was too small for hoop samples)
- Hoop residual stresses (evaluated using slit ring tests)

Table 2 shows the ratio between the maximum residual stress and the averaged yield stress for all the samples.

Sample	Max. residual stress / yield stress
1	0.38
2	0.39
3	0.39
4	0.47
5	0.47
6	0.49

Table 2. Measured residual stresses

2.3 Experimental facility

In Fig. 5 we present a scheme of the experimental set-up. The specimen was placed in a stiff pressure vessel, where it was loaded with external pressure with a pump. In order to measure the internal volume variation perforated end-caps were welded to the pipes. Each specimen was completely filled with water before the beginning of the test. From the hole in one of the end caps the water was directed to a container connected to a load cell. The load variation in the load cell is proportional to the displaced water.

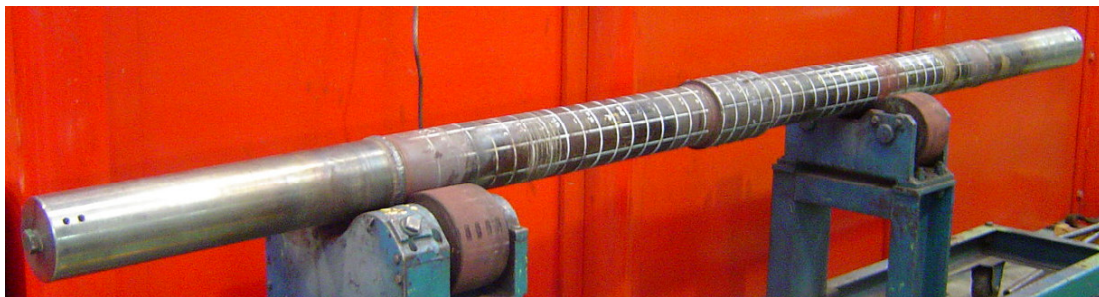
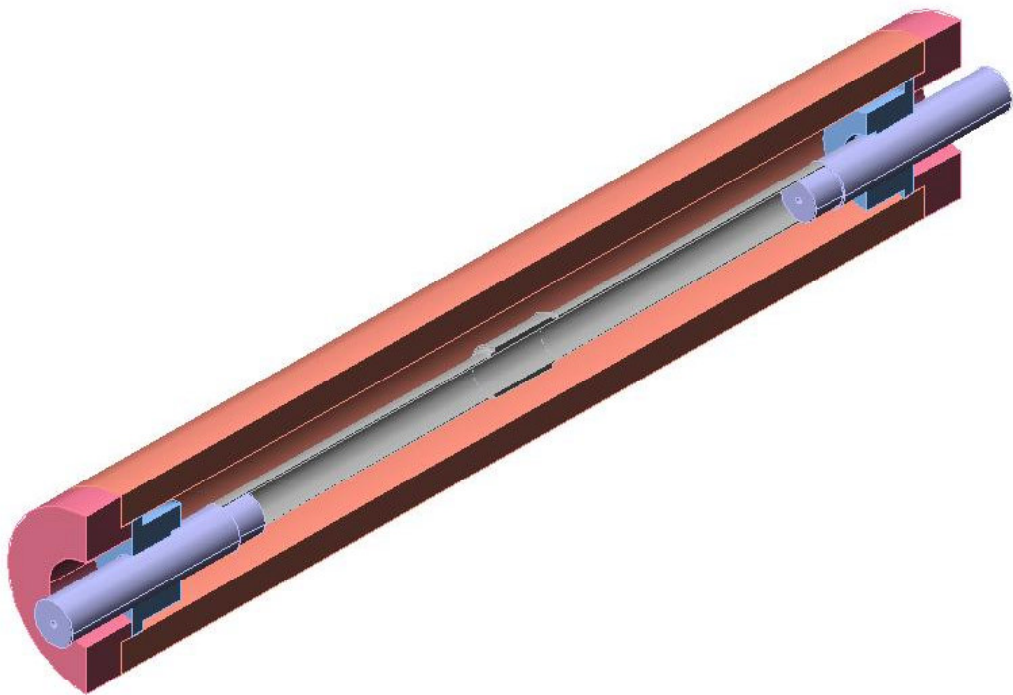
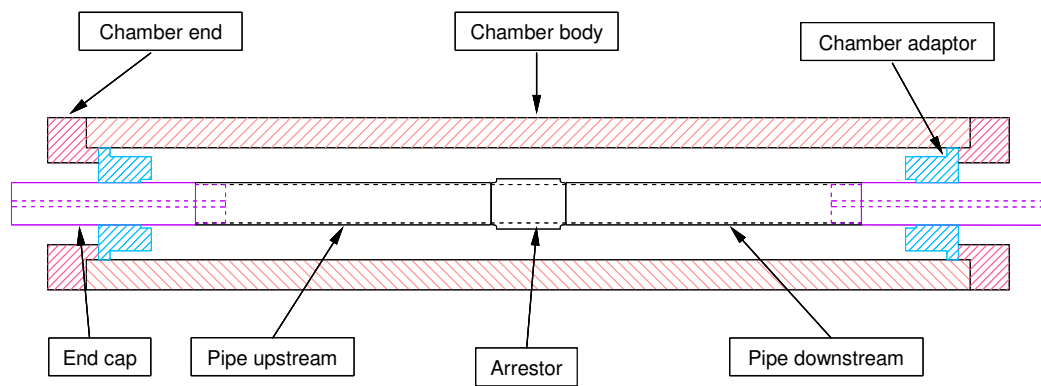


Figure 5. Experimental set-up.

2.4 Experimental results

Signals from a pressure transducer (pressure in the collapse vessel), and from the load cell were amplified, digitized and acquired in a PC with an “ad-hoc” program written for a LabView DAQ system. Coordinated pressure-time and volume-time records were stored and a volume-pressure curve could be plotted. A typical pressure-volume curve is shown in Fig. 6.

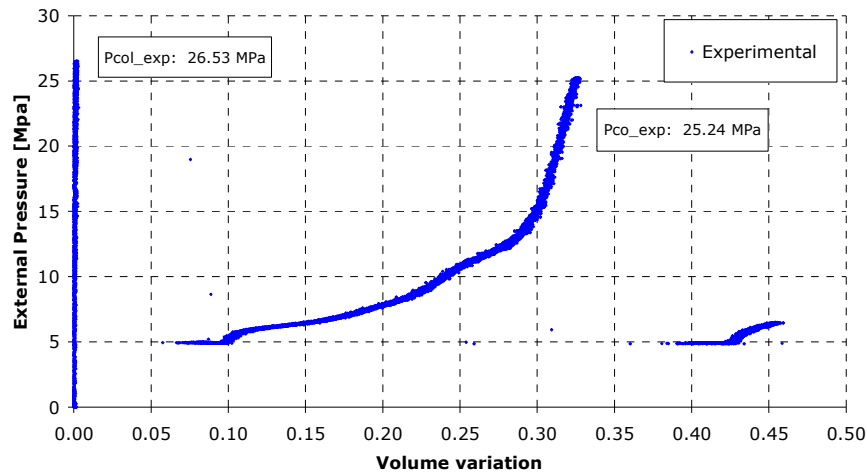


Figure 6. Experimentally determined p-V curves. (Sample5)

We use:

$$Volume\ variation = \frac{\Delta inside\ volume}{Original\ inside\ volume} \quad (1)$$

Figure 7 shows one of the samples after the test.



Figure 7. Sample 2 after test

Table 3 summarizes the experimental results:

Sample	Collapse pressure [MPa]	Crossover pressure [MPa]
1	29.50	Not reached ⁽¹⁾
2	29.03	11.89
3	28.02	21.17
4	27.37	16.48
5	26.53	25.24
6	28.47	27.45

Table 3. Experimental results

⁽¹⁾ The test was interrupted at 3737 psi and the crossover was not reached.

3 THE FINITE ELEMENT MODELS

For the numerical simulation of the crossing of an integral ring arrestor by a quasi-statically propagating buckle, we developed a finite element model using the MITC4 shell element in the ADINA general-purpose code. (Dvorkin and Bathe, 1984; ADINA SYSTEM)

The numerical model was developed using a material and geometrical nonlinear formulation, taking into account large displacements/rotations but small strains (Bathe, 1996) and it incorporated the following features:

- Geometry as described by the O.D. mapping and by the thickness distribution that was acquired for each sample as reported above.
- Von Mises elasto-plastic material model with isotropic multilinear hardening.
- Hoop residual stresses.
- Contact elements on the pipe inner surface in order to prevent its inter-penetration in the post collapse and propagation regime.
- Nonlinear equilibrium path tracing via the algorithm developed in Ref. Bathe and Dvorkin, 1983
- Residual stresses modeled with the technique discussed in Assanelli et al. 2000.

The mesh used to discretize the problem is shown in Fig. 8. The whole configuration analyzed consisted of an upstream pipe of length L_1 , an arrestor length L_a and a downstream pipe of length L_2 . The lengths L_1 and L_2 are determined according to the collapse chamber and arrestor dimensions.

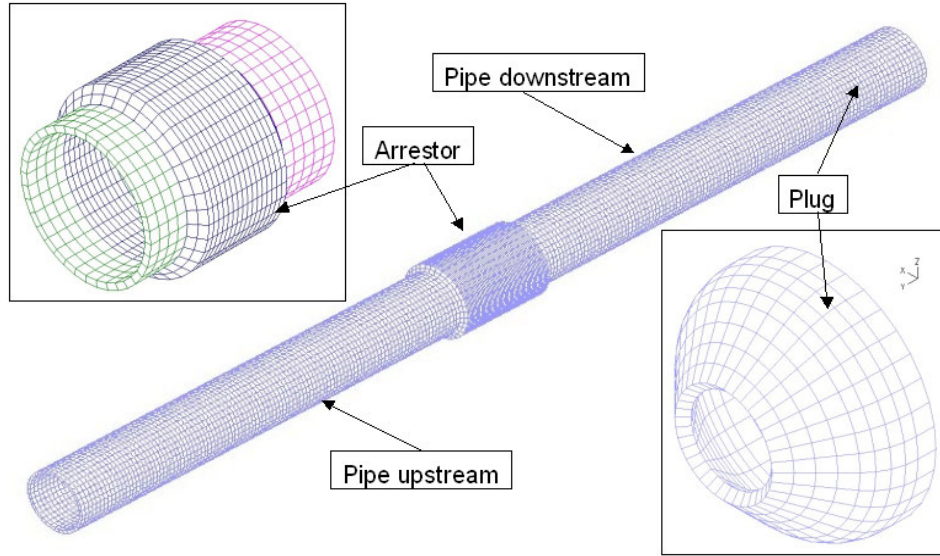


Figure 8. Finite element mesh of the sample.

For samples 4 to 6 a new design of the cap end with a special cone was introduced to avoid the pipe failure and consequently, we built a mesh of this cone with shell elements and we put contact surfaces between the cone and the inner surfaces of the pipe. The mesh of the cone is also shown in figure 8. As regards the cylindrical part of the plug we put a skew system on the extreme nodes of the pipe and we fixed the radial, tangential and axial displacements at $x=0$, and the radial and tangential displacements at $x=L$, allowing the tube to expand in the X-direction. The turns were left free.

Figures 9 and 10 show the actual engineering stress-strain curves recorded at our lab and its correspondent stress-strain curve used in the numerical model for some of the samples. Similar curves, based on our lab measurements, were used for the rest of them.

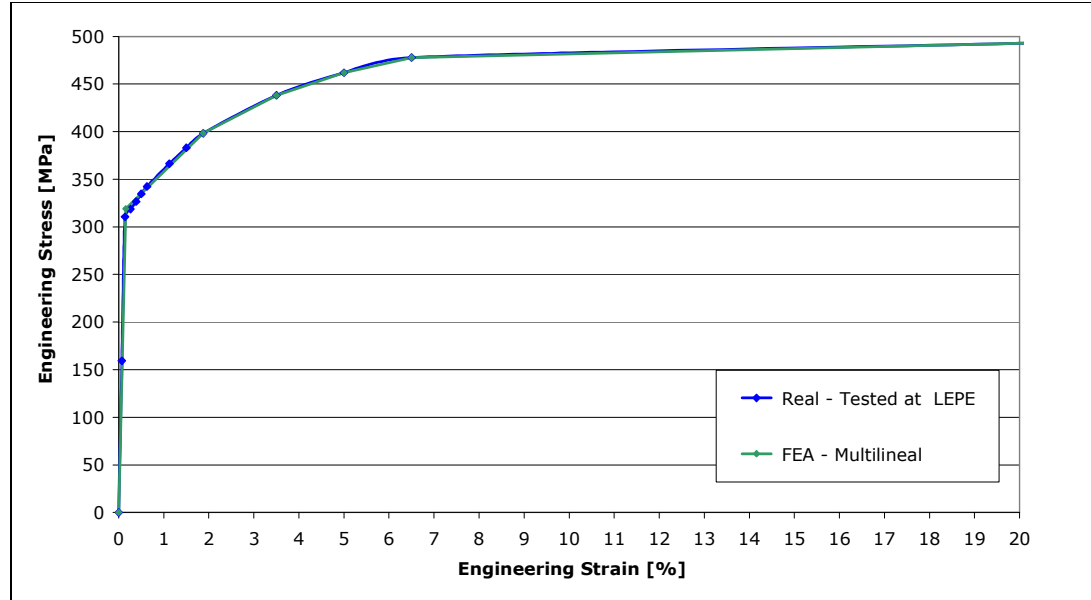


Figure 9: Material model for samples 2 and 3, actual and numerical curves.

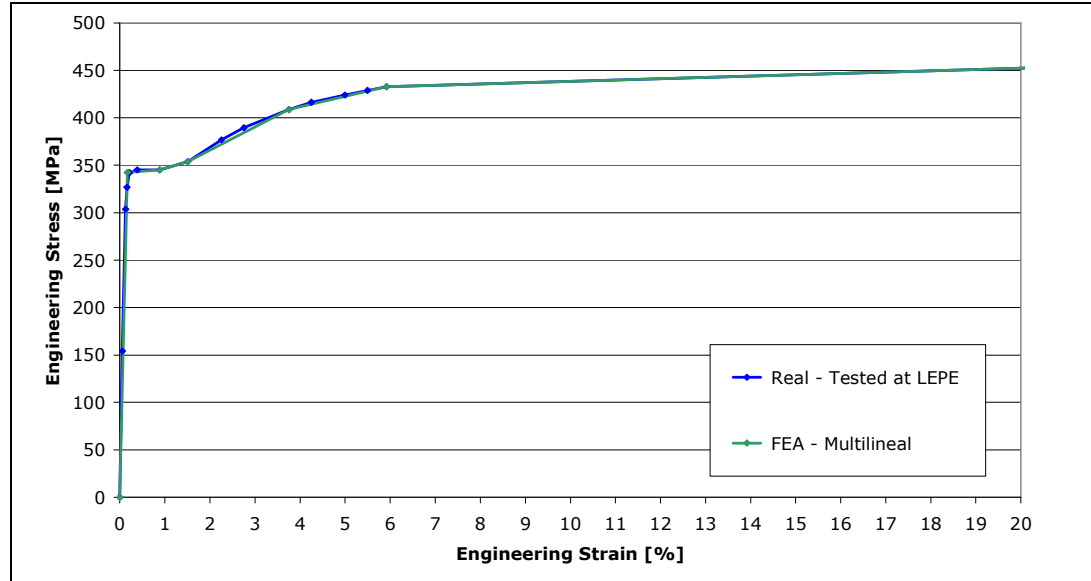


Figure 10: Material model for arrestors of samples 1 to 3, actual and numerical curves.

3.1 Identifying the different cross-over mechanisms

In Figures 11 and 12 we present the finite element predicted deformed shapes for a (pipes – arrestor) system exhibiting a flattening cross-over mechanism and a flipping cross-over mechanism. A simplified model, taking in account symmetry conditions, was used for these simulations.

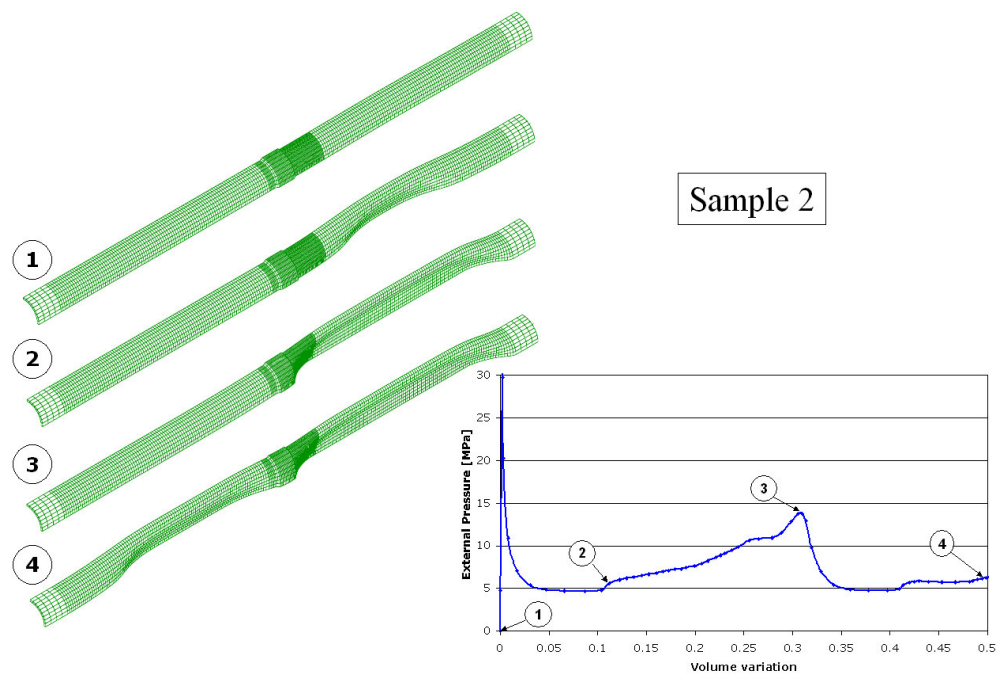


Figure 11. Sample 2: Flattening cross-over mechanism.

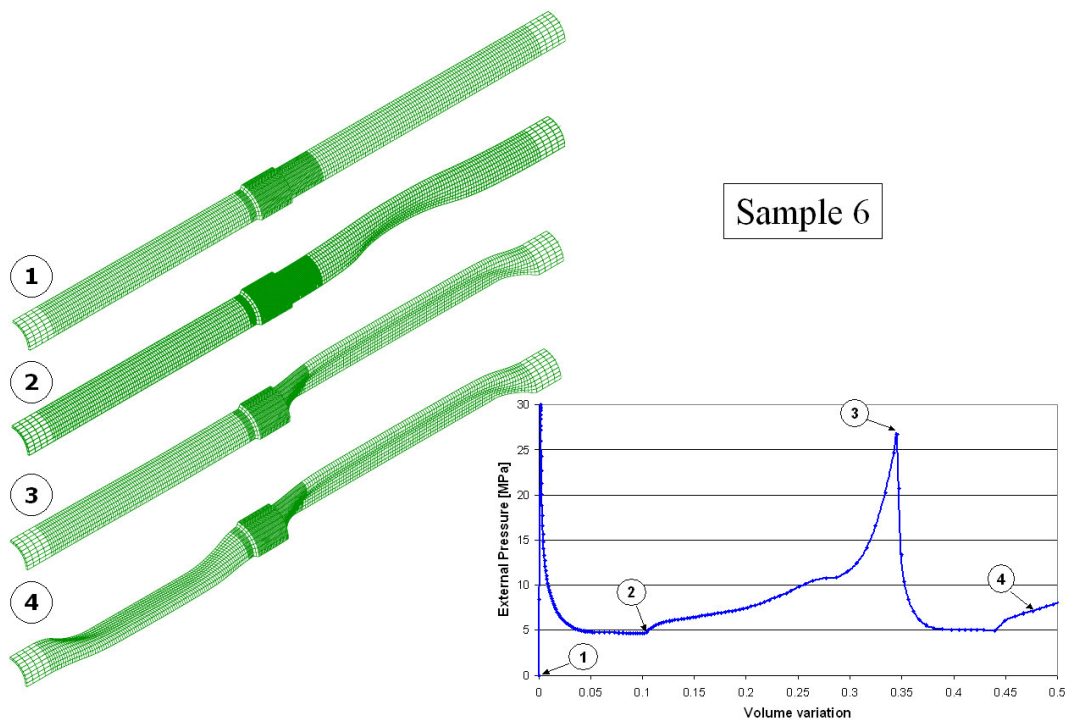


Figure 12. Sample 6: Flipping cross-over mechanism.

3.2 Validation of the Finite Element Results Using the Experimental Results

In Figure 13 we compare, for one of the samples, the experimentally determined and FEA predicted equilibrium paths and in figure 14, we show the deformed FE mesh after the analysis for the same sample.

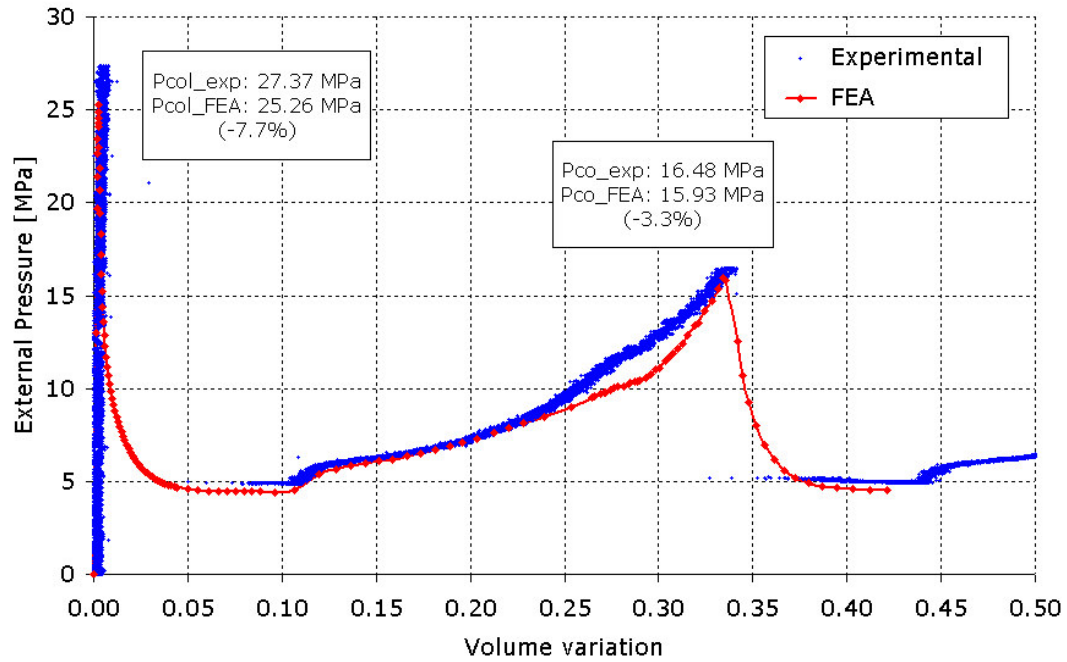


Figure 13. FEA vs. experimental results: flattening. (Sample 4)

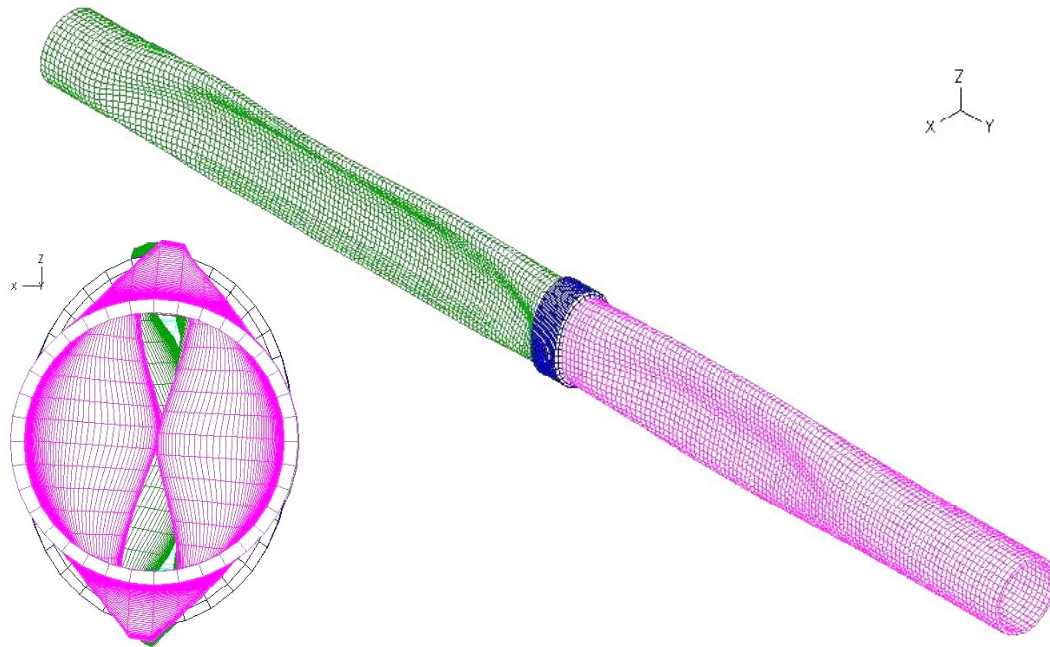


Figure 14. Finite element mesh of sample 4 after the crossover.

In figure 15 we compare the experimentally observed and the FEA predicted shape of the same sample after crossover.

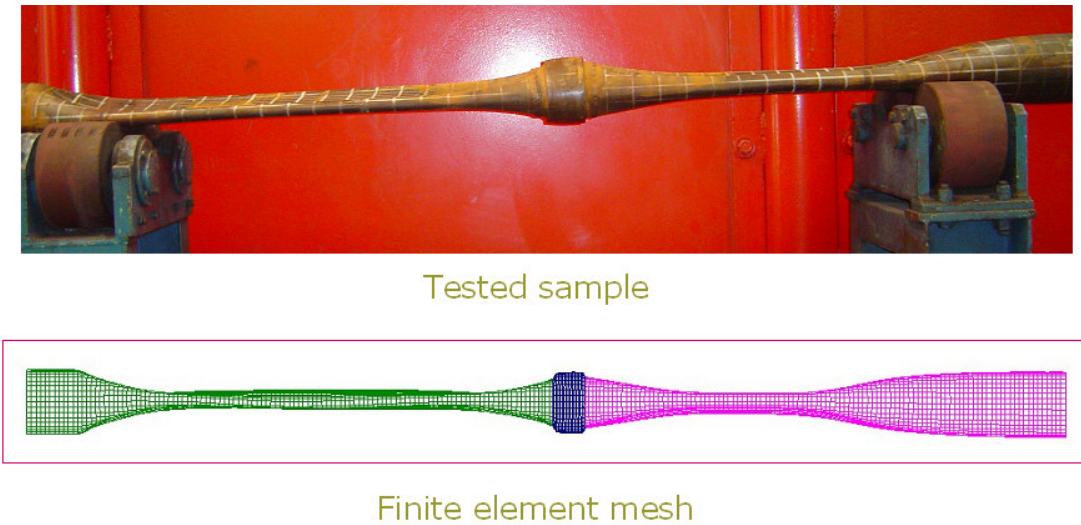


Figure 15. Experimentally observed and FEA predicted shapes of sample 4 after cross-over.

Figure 16 shows the comparison between the experimental and numerical pressure vs. volume variation responses for other sample. (Sample 6)

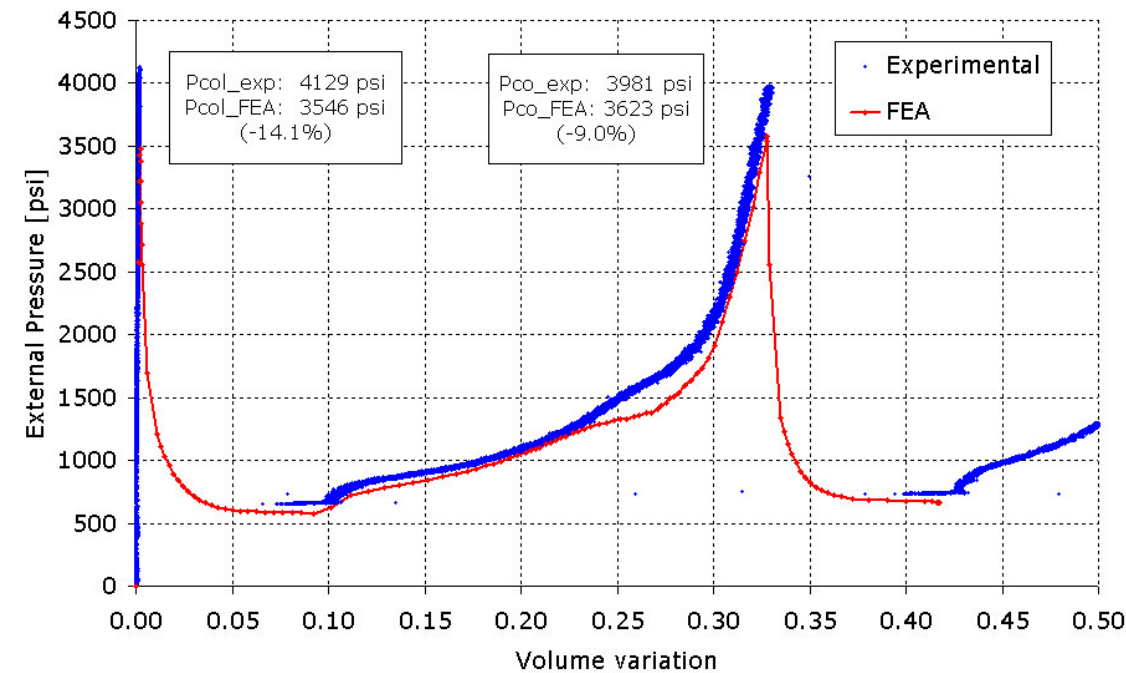


Figure 16. FEA vs. experimental results: flipping. (Sample 6)

Finally, in Figure 17 we show the deformed FE mesh after crossover and in figure 18 we compare the experimentally observed and FEA predicted shapes for sample 6.

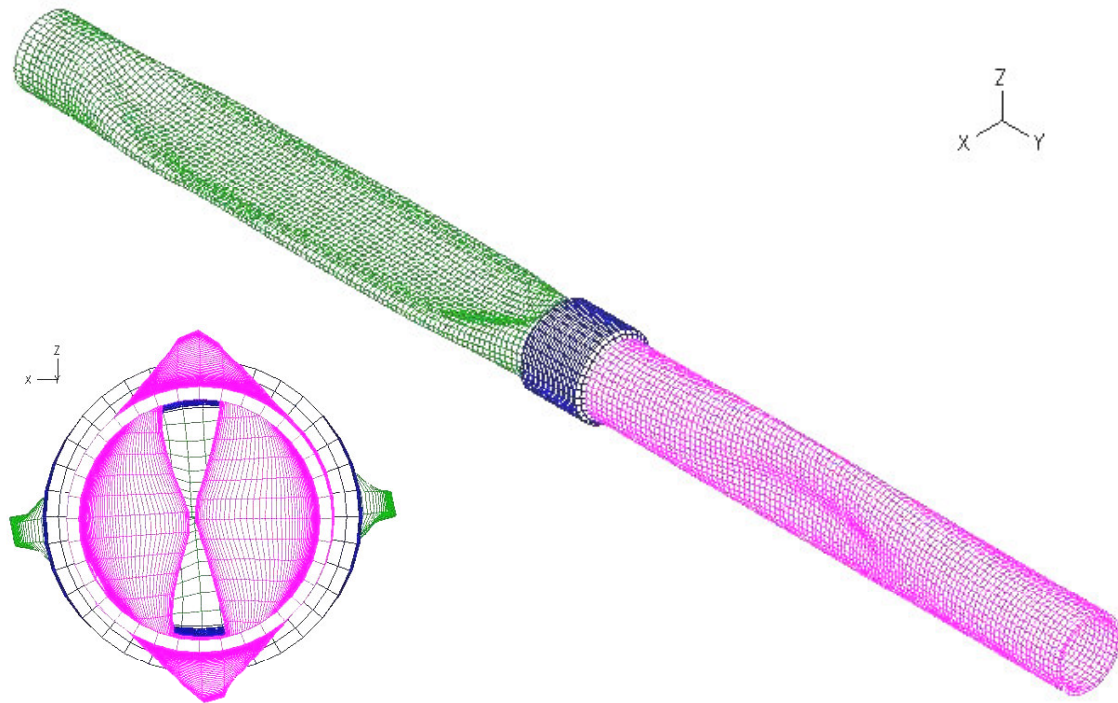
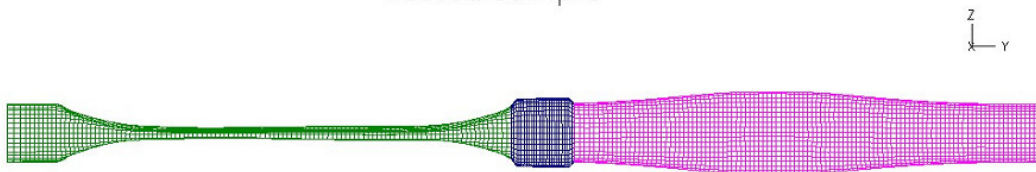


Figure 17. Finite element mesh of sample 6 after the crossover.



Tested sample



Finite element mesh

Figure 18. Experimentally observed and FEA predicted shapes of sample 6 after cross-over.

Table 4 compares all the FEA results with the experimental ones:

Sample	Collapse pressure: FEA/lab	Cross-over pressure: FEA/lab	$\eta = \frac{P_{co} - P_p}{P_{col} - P_p}$	Cross-over mode
1	0.946	Not reached	--	--
2	0.921	1.006	0.255	Flattening
3	0.969	1.105	0.643	Flattening
4	0.923	0.967	0.469	Flattening
5	0.953	0.927	0.848	Flipping
6	0.859	0.910	0.944	Flipping

Table 4. FEA vs. Experimental results

Where:

η is the efficiency of the arrestor ([Park and Kyriakides, 1997](#))

P_{co} is the crossover pressure

P_p is the propagation pressure

P_{col} is the collapse pressure

The flipping mode occurs for samples with high crossover pressures and consequently, at high efficiency levels. According with the literature ([Park and Kyriakides, 1997](#)) the transition between the flattening and the flipping mode is around 0.7 of efficiency, which is also observed in our experiments.

It is important to point out that the finite element results indicated in the previous table were obtained considering that the residual stresses in the two pipe sections are the residual stresses measured in the full length pipe. The modifications in residual stresses induced by the pipe cutting, the welding and groove machining were not considered in the model, this results in numerically predicted collapse pressures lower than the actual ones.

Figure 19 shows the high sensibility of the collapse pressure to the residual stresses introduced in our models. (We considered constant residual stress along the entire pipe)

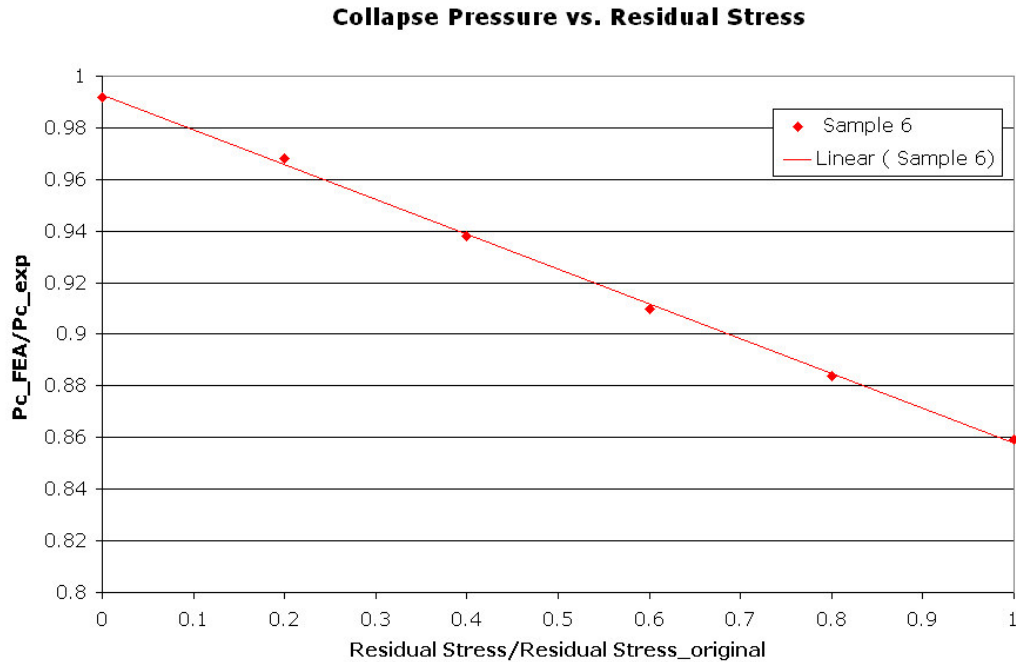


Figure 19. Variation of collapse pressure with the residual stress for sample 6.

4 CONCLUSIONS

A 3D finite element model was developed in order to be able to analyze the behavior of an integral ring buckle arrestor crossed over by a propagating buckle. The model was validated by comparing the numerical predictions with experimental determinations.

The model is able to simulate both, the flipping and the flattening cross-over mechanisms. (Park and Kyriakides, 1997)

The agreement between the finite element predictions and the laboratory observations, both for the collapse and cross-over pressure, is very good; hence, finite element models can be used as a reliable engineering tool to assess the performance of integral ring buckle arrestors for steel pipes.

5 REFERENCES

- The ADINA SYSTEM, ADINA R&D, Watertown, MA, U.S.A.
- A.P. Assanelli, R.G. Toscano, D.H. Johnson and E.N. Dvorkin, "Experimental / numerical analysis of the collapse behavior of steel pipes", *Engng. Computations*, **17**, pp.459-486, 2000.
- K.J. Bathe, *Finite Element Procedures*, Prentice Hall, NJ, 1996.
- K.J. Bathe and E.N. Dvorkin, "On the automatic solution of nonlinear finite element equations", *Computers & Structures*, **17**, pp.871-879, 1983.
- E.N.Dvorkin and K.J.Bathe, "A continuum mechanics based four-node shell element for general nonlinear analysis", *Engng. Computations*, **1**, pp. 77-88, 1984.
- T.G. Johns, R.E. Mesloh and J.E. Sorenson, "Propagating buckle arrestors for offshore pipelines". *ASME Journal of Pressure Vessel Technology*, **100**, pp. 206-214, 1978.
- S. Kyriakides, T.D. Park and T.A. Netto, "On the design of Integral Buckle Arrestors for

- Offshore Pipelines", *International Journal of Applied Ocean Research*, **20** pp.95-104, 1998.
- C.G. Langer, "Buckle arrestors for Deepwater Pipelines", *Proceedings of the Offshore Technology Conference*, OTC 10711, Houston, TX, U.S.A., 1999.
- T.A. Netto and S.F. Estefen, "Buckle Arrestors for Deepwater Pipelines", *International Journal of Marine Structures*, **9** pp.873-883, 1996.
- T.A. Netto and S. Kyriakides, "Dynamic performance of integral buckle arrestors for offshore pipelines. Part I: Experiments", *International Journal of Mechanical Sciences*, **42** pp.1405-1423, 2000a.
- T.A. Netto and S. Kyriakides, "Dynamic performance of integral buckle arrestors for offshore pipelines. Part II: Analysis", *International Journal of Mechanical Sciences*, **42** pp.1425-1452, 2000b.
- A.C. Palmer and J.H. Martin, "Buckle propagation in submarine pipelines", *Nature*, **254**, pp. 46-48, 1975.
- T.D. Park and S. Kyriakides, "On the performance of Integral Buckle Arrestors for Offshore Pipelines", *International Journal of Mechanical Sciences*, **39** pp.643-669, 1997.
- R.G. Toscano and E.N. Dvorkin, "Collapse and post-collapse behavior of steel pipes", Fifth World Congress on Computational Mechanics, Viena, Austria, July 2002.
- R.G. Toscano, M. Gonzalez and E.N. Dvorkin, "Validation of a finite element model that simulates the behavior of steel pipes under external pressure", *The Journal of Pipeline Integrity*, **2**, pp.74-84, 2003a.
- R.G. Toscano, M. Gonzalez and E.N. Dvorkin, "Experimental validation of a finite element model that simulates the collapse and post-collapse behavior of steel pipes", *Proceedings Second MIT Conference on Computational Fluid and Solid Mechanics*, (Ed. K.-J. Bathe), Elsevier, 2003b.
- R.G. Toscano, C. Timms, E.N. Dvorkin and D. DeGeer, "Determination of the collapse and propagation pressure of ultra-deepwater pipelines", *Proceedings OMAE 2003 - 22nd. International Conference on Offshore Mechanics and Arctic Engineering*, Cancun, Mexico, 2003c.
- R.G. Toscano, L. Mantovano and E.N. Dvorkin, "On the numerical calculation of collapse and collapse propagation pressure of steel deep water pipelines under external pressure and bending: Experimental verification of the finite element results", *Proceedings 4th. International Conference On Pipeline Technology*, pp. 1417-1428, Ostend, Belgium, 2004.

